

Ionization and Dissociation Energies of Group 13 Metal Complexes with Group 15 Hydrides

Shenggang Li, Gretchen K. Rothschof, Bradford R. Sohnlein, and Dong-Sheng Yang*

Department of Chemistry, University of Kentucky, Lexington, Kentucky 40506-0055

Received: March 6, 2002; In Final Form: June 3, 2002

In this work, 1:1 complexes of the group 13 metal atoms with the group 15 hydrides are prepared with laser-ablation molecular beam techniques and studied with threshold photoionization and zero electron kinetic energy photoelectron spectroscopies and ab initio calculations. Ionization energies of the $M-EH_3$ ($M = Al, Ga, In$; $E = N, P, As$) complexes increase in the order $N < P \leq As$, whereas bond dissociation energies decrease down the group 15 hydrides. For a given hydride, the ionization and dissociation energies are different among the three metals, though the variation is smaller than that of the ligand effect. Ionization enhances the binding between the metal and ligand, and the enhancement is as large as three to five times.

I. Introduction

Complexes of the group 13 metal atoms with the group 15 hydrides have been a subject of recent experimental and theoretical studies. They have been investigated as precursors for insertion and dehydrogenation products and as being relevant to chemical vapor deposition processes of the III–V semiconductor materials. Himmel et al. studied photoactivation of $M-NH_3$ and $M-PH_3$ ($M = Al, Ga, In$) using IR and UV–visible spectroscopies in argon matrices.^{1–3} They found that upon 436 nm irradiation the metal atom inserted into an N–H bond of ammonia to form the divalent compound of $HMNH_2$ and into P–H bonds of phosphine to form the divalent and trivalent compounds of $HMPH_2$ and H_2MPH . Imura et al. determined the permanent dipole moment of $Al-NH_3$ using the electrostatic hexapole method,⁴ Howard et al. measured magnetic properties of $Al-(NH_3)_2$ using electron paramagnetic resonance spectroscopy,⁵ Di Palma et al. recorded ionization thresholds of $M-NH_3$ ($M = Al, Ga, In$) by photoionization efficiency spectroscopy,^{6,7} Jakubek and Simard measured resonant two-photon ionization spectra of $Al-ND_3$,⁸ and our group investigated vibrationally resolved electronic spectra of $M-NH_3$ ($M = Al, Ga, In$) with zero electron kinetic energy (ZEKE) photoelectron spectroscopy.^{9–11} Theoretically, Davy and Jaffrey,¹² Sakai,¹³ Jursic,¹⁴ and Fängström et al.¹⁵ calculated the complexation energy of $Al-NH_3$ and the energy barrier for the Al insertion into an N–H bond to form $HAlNH_2$, using various ab initio methods including HF, B3LYP, MP2, MP4, CBS, QCISD, and CCSD(T). Stöckigt,¹⁶ Sodupe and Bauschlicher,¹⁷ Alcamí et al.,¹⁸ and Smith et al.¹⁹ predicted the bond dissociation energy of Al^+-NH_3 , also at different levels of theory. The bond energy of Al^+-NH_3 was calculated to be stronger than that of the corresponding neutral.

There has been little information, however, about the ionization and dissociation energies of the group 13 metal atoms (Al, Ga, In) with the group 15 heavy hydrides (PH_3, AsH_3), except for the theoretical predictions of the $Al-PH_3$ binding.^{13,20} In this article, we report a systematic study of the ionization energies (IEs) of $M-EH_3$ ($M = Al, Ga, In$; $E = N, P, As$) and the metal–ligand bond dissociation energies of $M-EH_3$ and

M^+-EH_3 , using threshold photoionization and ZEKE photoelectron spectroscopies and ab initio calculations. The IEs of the ammonia adducts were measured previously and are included for comparison. We have found that the coordination of the metal atoms with the hydrides reduces the IEs of the metals, and the reduction is greater with ammonia than with phosphine and arsine. The dissociation energies decrease down the group 15 hydrides, whereas differences among the group 13 metals are less dramatic with respect to the ligand effect.

II. Experimental and Computational Methods

The apparatus has been described in detail in a previous publication.¹⁰ It consists of a Smalley-type cluster source²¹ and a two-field space-focused Wiley–McLaren time-of-flight mass spectrometer.²² The spectrometer is housed inside a double-walled μ -metal cylinder and used for both ion and ZEKE electron detection.

Metal complexes were prepared by reactions of metal atoms with phosphine or arsine (99.999%, Matheson). The metal atoms were produced by pulsed laser vaporization of a pure metal rod (Al, 99.999%; In, 99.999%; Aldrich) or an alloy target (GaSb, 99.99%, Aldrich) with the laser wavelength of 532 nm and the pulse energy of ~ 4 mJ (Quanta-Ray, GCR-3). Phosphine or arsine was mixed with helium gas (Scott-Gross, UHP) at a concentration of 2–5% and a total pressure of 60 psi. The mixture was then pulsed into the vaporization chamber, and the gas pulses were synchronized with laser pulses.

Complexes were ionized with UV photons from a frequency-doubled dye laser (Lumonics, HD-500), which was pumped by a XeCl excimer (Lumonics, PM-884). Their masses were determined with the time-of-flight mass spectrometer. Ionization thresholds were located by recording the mass-selected ion signal as a function of laser wavelengths. The ZEKE signal was produced by photoexcitation, followed by delayed, electric field ionization. The ion and ZEKE signals were detected with a dual microchannel plate (Galileo), amplified with a preamplifier (Stanford Research, SR445), averaged with a gated integrator (Stanford Research, SR250), and stored in a laboratory computer. Electric pulses of 100 ns and 1.2 V cm^{-1} were supplied by a delay pulse generator (Stanford Research, DG535). Laser wavelengths were calibrated with titanium atomic transitions.²³

* Corresponding author. E-mail: dyang0@uky.edu.

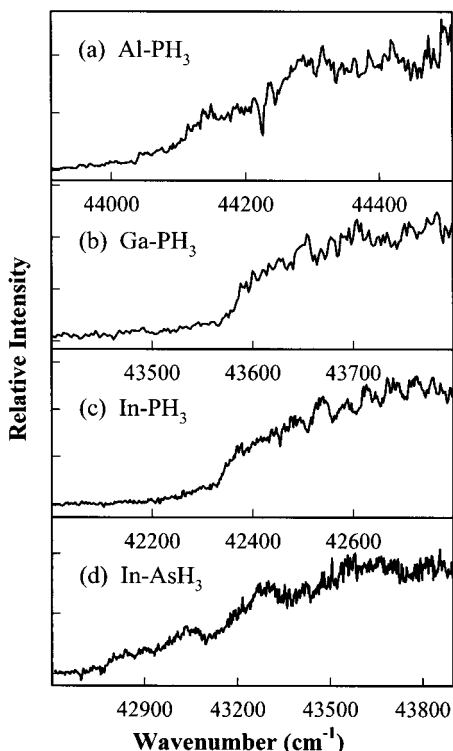


Figure 1. Threshold photoionization spectra of $M\text{-PH}_3$ ($M = \text{Al, Ga, In}$) and In-AsH_3 . The wavenumbers are corrected for the field ionization effect.

Geometry optimization and vibrational analysis were performed with Gaussian 98 computational software.²⁴ Vibrational analysis was carried out to ensure the global minimum was located in the geometry optimization and to calculate zero point vibrational energies. For Al-NH_3 , we carried out calculations with B3LYP, MP2, MP4(STDQ), CISD, QCISD, and CCSD(T) methods and 6-311+G(d,p), D95+(d,p), and AUG-cc-pVDZ basis sets. For all other complexes, we performed only B3LYP/6-311+G(d,p) calculations. Because the triple-split valence basis is not available for indium, the Los Alamos ECP plus DZ basis (LANL2DZ) was used for this metal atom. IEs and dissociation energies were corrected for zero point vibrational energies from the vibrational analysis.

III. Results and Discussion

A. Spectroscopy. Figure 1 shows the threshold photoionization spectra of $M\text{-PH}_3$ ($M = \text{Al, Ga, In}$) and In-AsH_3 . An electric field of 320 V cm^{-1} was applied in the laser ionization region, and this external field is expected to introduce a red shift of ionization threshold by about 110 cm^{-1} [$\Delta E (\text{cm}^{-1}) = 6.1 F(\text{V cm}^{-1})^{1/2}$].²⁵ With the correction of the field effect, the ionization thresholds are measured to be $44050 (100) \text{ cm}^{-1}$ for Al-PH_3 , $43550 (100) \text{ cm}^{-1}$ for Ga-PH_3 , $42300 (100) \text{ cm}^{-1}$ for In-PH_3 , and $42750 (200) \text{ cm}^{-1}$ for In-AsH_3 . We tried reactions of Al and Ga with AsH_3 , however, no ionized 1:1 complexes were observed under our experimental conditions. The Al-AsH_3 and Ga-AsH_3 adducts should be formed in the molecular beams because they are predicted to be more strongly bound than In-AsH_3 . It is likely that the IEs of these complexes are higher than the laser energy (5.55 eV) used in the measurements.

Figure 2 displays ZEKE spectra of Ga-PH_3 and In-PH_3 . In both cases, the ZEKE signals are very weak, and the spectra exhibit only one major peak with a width of about 10 cm^{-1} . The peak positions are $43545(5) \text{ cm}^{-1}$ for Ga-PH_3 and $42319-$

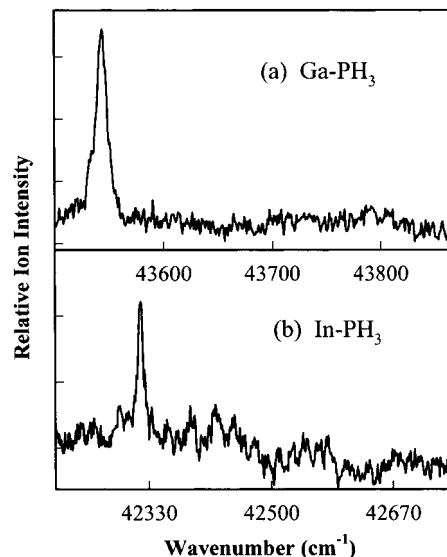


Figure 2. Zero electron kinetic energy photoelectron spectra of Ga-PH_3 and In-PH_3 .

$5) \text{ cm}^{-1}$ for In-PH_3 . These values match the ionization thresholds measured from the photoionization spectra, but with much higher accuracy. We were unable to obtain ZEKE spectra for Al-PH_3 and In-AsH_3 . The Al-PH_3 and In-NH_3 complexes are predicted to have larger geometry changes than Ga-PH_3 and In-AsH_3 upon ionization. The large geometry variations lead to slow onsets in the photoionization efficiency curves of the two complexes (Figure 1a and d), which contribute to the difficulty in observing the ZEKE signal.

B. Computation. Because there has been very limited computational work on the IEs of metal–ligand complexes, we have performed a rather comprehensive investigation with a range of electronic structure models and basis sets for the aluminum–ammonia complex. The purpose of the systematic study is to find a best suitable method for the titled molecular systems. The theoretical models used in this work include density functional theory (B3LYP), Møller–Plesset perturbation (MP2, MP4), configuration interaction (CISD, QCISD), and coupled cluster (CCSD(T)) methods. The basis sets cover Pople style 6-311+G(d,p), Dunning–Huzinaga D95+(d,p), and Dunning’s correlation-consistent AUG-cc-pVDZ. Figure 3 summarizes the calculated IEs in comparison with the experimental value. It shows that the B3LYP calculations yield IEs within 600 cm^{-1} of the measured value (39746 cm^{-1}), whereas other methods give a difference up to 2200 cm^{-1} . In addition, the correlation-consistent basis yields the best results with the electron correlation models, whereas all the three basis functions give rather similar IEs with B3LYP. The good performance of the B3LYP method may result from the cancellation of the errors in the density functional method and the basis set convergence.²⁶ With considerations of the quality and efficiency of the computation models and the availability of the basis sets for heavy atoms in the Gaussian 98 software, we have chosen the B3LYP/6-311+G(d,p) method for the $M\text{-EH}_3$ complexes.

Table 1 presents the adiabatic IEs, vibrational frequencies, and dissociation energies calculated from the B3LYP/6-311+G(d,p) method. In comparison with the experimental values, the errors in metal–ligand stretching frequencies are less than 9%, whereas the differences in IEs are smaller than 2%. The theoretical errors seem to be random so that any scaling procedure will not improve their accuracies. Nevertheless, the calculated IEs and vibrational frequencies are in good agreement with the measured values, though the calculations do not yet

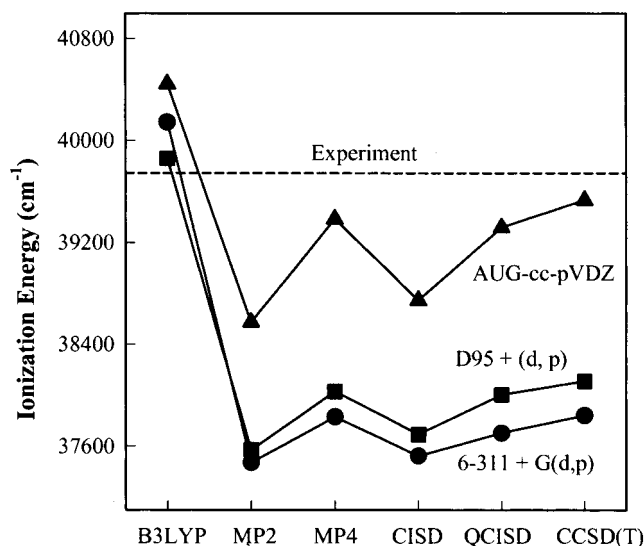


Figure 3. Ionization energies of Al–NH₃ from ZEKE measurements (dashed line) and various ab initio calculations with the 6-311+G(d,p) (circles), D95+(d,p) (squares), and AUG-cc-pVDZ (triangles) basis functions.

TABLE 1: IEs (eV),^a Metal–Ligand Stretching Frequencies (cm⁻¹), and Bond Dissociation Energies (kcal mol⁻¹) of M–EH₃ and Bond Energy Differences between M–EH₃ and M⁺–EH₃ (M = Al, Ga, In; E = N, P, As)

molecule	IE (eV)		ν_s/ν_s^+ (cm ⁻¹)		D_0/D_0^+ (kcal mol ⁻¹)		$\Delta(D_0^+ - D_0)$ (kcal mol ⁻¹)	
	ZEKE	B3LYP	ZEKE	B3LP	B3LYP	ZEKE	B3LYP	
Al–NH ₃ ^b	4.928	4.98	227/339	217/309	9.3/33.2	24.4	23.9	
Al–PH ₃	5.46 ^c	5.41		135/186	4.7/18.6	12.1	13.9	
Al–AsH ₃		5.45		104/156	3.4/16.3		12.9	
Ga–NH ₃ ^c	4.976	5.02	161/270	174/266	7.8/31.0	23.6	23.2	
Ga–PH ₃	5.398	5.40		111/159	4.8/19.3	13.8	14.5	
Ga–AsH ₃		5.45		77/118	3.7/17.1		13.4	
In–NH ₃ ^d	4.921	4.83	141/234	153/234	6.8/28.9	19.9	22.1	
In–PH ₃	5.247	5.14		71/130	3.1/16.9	12.4	13.8	
In–AsH ₃	5.30 ^e	5.20		50/94	2.3/14.8	11.2	12.5	

^a Adiabatic IEs except for those from threshold photoionization. ^b Reference 9. ^c Reference 11. ^d Reference 10. ^e From threshold photoionization. ^f ν_s/ν_s^+ stretching frequencies of the neutral/ion. ^g D_0/D_0^+ dissociation energies of the neutral/ion.

achieve spectroscopic accuracy. For metal–ligand bond energies, experimental measurements are not available to evaluate the quality of the B3LYP calculations. However, the B3LYP results can be compared with previous theoretical studies. The dissociation energies of Al–NH₃ were calculated to be 8.6 kcal mol⁻¹ at the CISD/TZ2P level,¹² 9.5 kcal mol⁻¹ at MP4/6-31+G(d,p)//HF/6-31G(d,p),¹³ 11.0 kcal mol⁻¹ at CBS-Q,¹⁴ and 13.0 kcal mol⁻¹ at CCSD(T)/6-31G(d,p)//QCISD/6-31G(d,p).¹⁵ The bond energies of Al⁺–NH₃ were predicted to be 32.5 kcal mol⁻¹ with the B3LYP/6-311++G(3df,2p)//6-311+G(d,p) method,¹⁶ 34.9 kcal mol⁻¹ by MCP/ANO,¹⁷ 41.8 kcal mol⁻¹ from MP4/6-31G(d),¹⁸ and 32.8 kcal mol⁻¹ at HF/6-31G(d).¹⁹ These calculations are compared to the values of 9.3 and 33.2 kcal mol⁻¹ for the neutral and ion obtained in this work. For Al–PH₃, the bond energies were calculated as 2.7 and 2.6 kcal mol⁻¹ with CISD/TZ2P¹² and MP4/6-31+G(d,p)//HF/6-31G(d,p),¹³ lower than the B3LYP/6-311+G(d,p) value of 4.7 kcal mol⁻¹. Clearly, the dissociation energies from various levels of theory span a wide range of values; experimental measurements are required to assess the accuracy of the theoretical predictions.

Although a direct comparison between theory and experiment is not possible for the bond energies of these complexes, the

calculated differences between the M–NH₃ and M⁺–NH₃ bond strengths can be compared to the spectroscopic measurements, as $IE(M) - IE(M-EH_3) = D_0^+(M^+-EH_3) - D_0(M-EH_3)$. This comparison is useful because it provides some measure of assessing the reliability of the bond energies calculated by the B3LYP method and is shown in Table 1. It can be seen from the table that the absolute differences range from 0.4 to –2.2 kcal mol⁻¹, which account for the relative errors of 2.0–15.0%. The best agreement between the theory and the experiment is for Al–NH₃ and Ga–NH₃, while the poorest is for Al–PH₃. The relative errors are similar for the three indium complexes.

C. Trends in Ionization and Dissociation Energies. The IEs of the M–EH₃ (M = Al, Ga, In; E = N, P, As) complexes are lower than that of the corresponding metal atoms [5.986 eV (Al), 5.999 eV (Ga), 5.786 eV (In)],²³ and shifts are substantially larger for M–NH₃ than for M–PH₃/AsH₃. The IE values of the complexes for a certain ligand are also different among the three metals, though the distinction is subtle. As noted above, the decrease in the IEs from the naked to the ligated metal is equal to the increase of the bond energies from the neutral to the ionized complex. The changes in the IEs and bond energies result from the additional charge-dipole/charge-induced dipole interactions in the ion and the removal of an antibonding electron from the neutral. In first approximation^{27,28} we may imagine these neutral complexes being formed mainly by the interaction of the M np with the EH₃ lone pair orbital. In this interaction, the M np electron may be oriented along the M–E axis or perpendicular to it. In the former case, a $\sigma^2\sigma^*$ configuration is formed, where the σ^2 orbital retains largely the EH₃ lone-pair character and the σ^* orbital is basically the M p σ . This type of interaction, however, yields a large electron repulsion because the M p σ electron points toward to the ligand electron lone-pair. In the latter case, a $\sigma^2\pi$ configuration is created with the π orbital being perpendicular to the M–E axis. The $\sigma^2\pi$ configuration should be more stable because of the reduced electron repulsion and the donation of the ligand electron lone-pair to the empty M p σ orbital. Thus, the ground electronic state of M–EH₃ is expected to be ²E in C_{3v} symmetry, which may undergo Jahn–Teller distortion and split into two nondegenerate ²A' and ²A'' states of C_s geometry. Our B3LYP/6-311+G(d,p) calculations predict a ²A' ground state for the M–NH₃ complexes and a ²A'' ground state for M–PH₃ and M–AsH₃. The highest occupied molecular orbital (HOMO) of M–EH₃ may be a pure M p π character or a mixture of the metal p π with a ligand orbital of an appropriate symmetry. If the HOMO were of pure metal character, the IE of the complex would be little shifted with respect to the metal atom. If the HOMO consists of a mixture of the M p π and a filled ligand e orbital which splits into a' and a'' under Jahn–Teller distorted C_s symmetry, the IE of the complex is expected to be lower than that of the metal atom. The IE reduction can arise from the destabilization of the HOMO, because the ligand orbital is lower in energy than M p π so that the mixing is in an antiphase manner about the M p π orbital. Such antibonding mixing is predicted in our calculations, as shown by the Al–NH₃ HOMO electron density map plotted with MOLDEN 3.7 (Figure 4).²⁹ Furthermore, an electron back-donation may occur from the M p π orbital to a low-lying empty ligand π orbital and stabilize the HOMO. Differential electronic properties among group 15 compounds have been observed in coordination chemistry.^{30–32} It has been known that phosphines and arsines have fairly low-lying empty orbitals acting as π acceptors, whereas there is no strong evidence of ammonia with similar property. Thus, the measured IEs between the metal–ammonia and metal–phos-

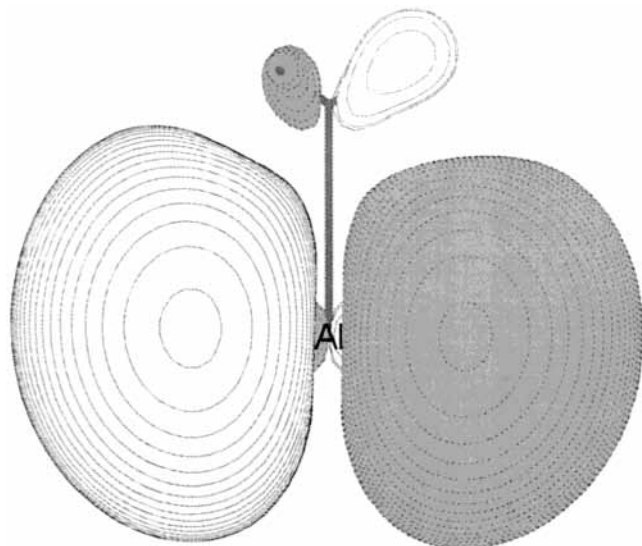


Figure 4. Highest occupied molecular orbital of Al–NH₃.

phine/arsine complexes may reflect the distinctive bonding properties of these ligands.

The dissociation energies of M–EH₃ decrease in the order of NH₃ > PH₃ ≥ AsH₃ for a given metal and Al > Ga > In for NH₃ and Al ~ Ga > In for PH₃ and AsH₃. The Al > Ga > In order correlates with the extent of orbital overlap and the magnitude of electron affinities of the metal atoms.²³ The bond energies of M⁺–EH₃ are about 3–5 times stronger than that of M–EH₃, but their trend is the same as in the corresponding neutrals. The binding strengths of M⁺–EH₃ are predicted to be similar to those of the MX₃–EH₃ complexes, where X is F, Cl, Br, I.³³ In these mono and trivalent complexes, the ammonia adducts are bound about twice as strongly as the phosphine and arsine association complexes. Timoshkin et al. analyzed electrostatic and covalent contributions to the binding in MX₃–EH₃ and concluded that while the electrostatic and covalent contributions were of the same order for the NH₃ adducts, the electrostatic contributions were negligible for PH₃ and AsH₃. The weaker electrostatic binding of the heavy hydrides is consistent with their smaller permanent dipole moments (0.574 D for PH₃, 0.2 D for AsH₃) with respect to ammonia (1.471 D).²³

IV. Conclusion

The adducts of the group 13 metal atoms with the group 15 hydrides have been studied with ab initio calculations, threshold photoionization, and ZEKE photoelectron spectroscopy. The IEs of the metal atoms decrease upon coordination with the hydrides. The IE shifts with ammonia coordination are about twice as large as those with phosphine and arsine, whereas the IE differences among the three metals are smaller. The dissociation energies follow the trend parallel to the IE shifts, with the metal–ammonia binding being the strongest. Among the three metals, the binding strengths are in the order of Al > Ga > In for ammonia and Al ~ Ga > In for the heavier hydrides. Upon ionization the metal–ligand binding increases by a factor of 3 to 5 depending on the hydrides. The trends in the ionization and dissociation energies are related to the orbital and electrostatic interactions.

Acknowledgment. The authors are grateful for the funding of this research by the National Science Foundation and the Petroleum Research Fund, administered by the American Chemical Society. G.K.R. acknowledges the award of a post-doctoral fellowship by the University of Kentucky Center for Computational Sciences.

References and Notes

- (1) Himmel, H.-J.; Downs, A. J.; Greene, T. M. *J. Am. Chem. Soc.* **2000**, *122*, 9793.
- (2) Himmel, H.-J.; Downs, A. J.; Greene, T. M. *Inorg. Chem.* **2001**, *40*, 396.
- (3) Himmel, H.-J.; Downs, A. J.; Green, J. C.; Greene, T. M. *J. Chem. Soc., Dalton Trans.* **2001**, 9793.
- (4) Imura, K.; Kawashima, T.; Ohoyama, H.; Kasai, T. *J. Am. Chem. Soc.* **2001**, *123*, 6367.
- (5) Howard, J. A.; Joly, H. A.; Edwards, P. P.; Singer, R. J.; Logan, D. E. *J. Am. Chem. Soc.* **1992**, *114*, 474.
- (6) Di Palma, T. M.; Latini, A.; Satta, M.; Varvesi, M.; Giardini, A. *Chem. Phys. Lett.* **1998**, *284*, 184.
- (7) Di Palma, T. M.; Latini, A.; Satta, M.; Giardini, A. *Eur. Phys. J. D* **1998**, *4*, 225.
- (8) Jakubek, J.; Simard, B. *J. Chem. Phys.* **2000**, *112*, 1733.
- (9) Yang, D. S.; Miyawaki, J. *Chem. Phys. Lett.* **1999**, *313*, 514.
- (10) Rothschof, G. K.; Perkins, J. S.; Li, S.; Yang, D. S. *J. Phys. Chem. A* **2000**, *104*, 8178.
- (11) Li, S.; Rothschof, G. K.; Pillai, D.; Sohnlein, B. R.; Wilson, B. M.; Yang, D. S. *J. Chem. Phys.* **2001**, *115*, 7968.
- (12) Davy, R. D.; Jaffrey, K. L. *J. Phys. Chem.* **1994**, *98*, 8930.
- (13) Sakai, S. *J. Phys. Chem.* **1992**, *96*, 8369.
- (14) Jursic, B. S. *Chem. Phys. Lett.* **1998**, *237*, 51.
- (15) Fängström, T.; Lunell, S.; Kasai, P. H.; Eriksson, L. A. *J. Phys. Chem. A* **1998**, *102*, 1005.
- (16) Stöckigt, D. *Chem. Phys. Lett.* **1996**, *250*, 387.
- (17) Sodupe, M.; Bauschlicher, C. W., Jr. *Chem. Phys. Lett.* **1991**, *181*, 321.
- (18) Alcamí, M.; M6, O.; Yáñez, M. J. *Mol. Struct. Theochem.* **1991**, *234*, 357.
- (19) Smith, S. F.; Chandrasekhar, J.; Jorgensen, W. L. *J. Phys. Chem.* **1983**, *87*, 1898.
- (20) Davy, R. D.; Schaefer, H. F., III. *J. Phys. Chem. A* **1997**, *101*, 3135.
- (21) Dietz, T. G.; Duncan, M. A.; Powers, D. E.; Smalley, R. E. *J. Chem. Phys.* **1981**, *74*, 6511.
- (22) Wiley, W. C.; McLaren, I. H. *Rev. Sci. Instrum.* **1955**, *26*, 1150.
- (23) Lide, D. R.; Frederikse, H. P. R. *CRC Handbook of Chemistry and Physics*, 78th ed.; CRC Press: New York, 1997.
- (24) Frisch, M. J.; Trucks, G. W.; Schlegel, H. B.; Scuseria, G. E.; Robb, M. A.; Cheeseman, J. R.; Zakrzewski, V. G.; Montgomery, J. A., Jr.; Stratmann, R. E.; Burant, J. C.; Dapprich, S.; Millam, J. M.; Daniels, A. D.; Kudin, K. N.; Strain, M. C.; Farkas, O.; Tomasi, J.; Barone, V.; Cossi, M.; Cammi, R.; Mennucci, B.; Pomelli, C.; Adamo, C.; Clifford, S.; Ochterski, J.; Petersson, G. A.; Ayala, P. Y.; Cui, Q.; Morokuma, K.; Malick, D. K.; Rabuck, A. D.; Raghavachari, K.; Foresman, J. B.; Cioslowski, J.; Ortiz, J. V.; Stefanov, B. B.; Liu, G.; Liashenko, A.; Piskorz, P.; Komaromi, I.; Gomperts, R.; Martin, R. L.; Fox, D. J.; Keith, T.; Al-Laham, M. A.; Peng, C. Y.; Nanayakkara, A.; Gonzalez, C.; Challacombe, M.; Gill, P. M. W.; Johnson, B. G.; Chen, W.; Wong, M. W.; Andres, J. L.; Head-Gordon, M.; Replogle, E. S.; Pople, J. A. Gaussian, Inc.: Pittsburgh, PA, 1998.
- (25) Duncan, M. A.; Dietz, T. G.; Smalley, R. E. *J. Chem. Phys.* **1981**, *75*, 2118.
- (26) Dunning, T. H. *J. Phys. Chem. A* **2000**, *104*, 9062.
- (27) Duval, M.-C.; Soep, B.; Breckenridge, W. H. *J. Phys. Chem.* **1991**, *95*, 7145.
- (28) Barckholtz, T. A.; Powers, D. E.; Miller, T. A.; Bursten, B. E. *J. Am. Chem. Soc.* **1999**, *121*, 2576.
- (29) Schaftenaar, G.; Noordik, J. H. *J. Comput.-Aided Mol. Des.* **2000**, *14*, 123.
- (30) Cotton, F. A.; Wilkinson, G.; Murillo, C. A.; Bochmann, M. *Advanced Inorganic Chemistry*, 6th ed.; Wiley: New York, 1999.
- (31) Davis, M. S.; Pierens, R. K.; Aroney, M. J. *J. Organomet. Chem.* **1993**, *458*, 141.
- (32) Marynick, D. S. *J. Am. Chem. Soc.* **1984**, *106*, 4064.
- (33) Timoshkin, A. Y.; Suvorov, A. V.; Bettingger, H. F.; Schaefer, H. F. *J. Am. Chem. Soc.* **1999**, *121*, 5687.